JOURNAL OF MATERIALS SCIENCE 32 (1997) 6055–6062

Study of the interfacial phenomena during friction surfacing of aluminium with steels

M. CHANDRASEKARAN, A. W. BATCHELOR, S. JANA
School of Mechanical and Production Engineering, Nanyang Technological University, Nanyang Avenue, Singapore 2263

Friction surfacing was carried out with stainless steel 304 and mild steel 1020 consumables on to an aluminium 5083 substrate in an argon atmosphere. Mild steel bonded well with the substrate and there was evidence of interfacial compound formation whereas in the case of stainless steel consumable there was no evidence of mixing and the coating was found to have a rolled structure on the surface. No clear evidence of mechanical interlock was obtained for stainless steel on aluminium. In both cases a nominal contact pressure as high as 21.8 MPa was required to obtain a good coating. For the mild steel coating there was evidence of transfer of aluminium on to the coating and the matrix had a shear crack along the matrix/coating interface.

1. Introduction

Surface engineering has gained wide importance owing to the advantages realized by it in materials technology. An important form of surface engineering is the friction surfacing technique. Friction surfacing, which is related to friction welding, utilizes the frictional energy dissipated during an operation and generates a layer of plasticized metal. The layer of plasticized metal is deposited as a coating without the need for an external heat source. In this process, the consumable is the rod of coating metal which moves relative to the substrate in a linear direction while rotating relative to the substrate under the action of external load. The friction surfacing was first patented as a metal-coating process in 1941 by Klopstock [1], but only recently has it been developed as a practical industrial process [3–7]. This process has been used for obtaining various dissimilar metal coatings such as tool steel coatings on mild steel or stainless steel on mild steel [8]. Dissimilar metal coatings are made possible by the generation of high contact stress and intimate contact between the coating material and the substrate which initiates solid-state adhesion between coating and substrate [7]. Strong bonding is achieved between the coating and the substrate in a friction surfacing process if a high contact pressure is used which requires expensive equipment [2, 8].

A major parameter in determining the economy of the process is the contact pressure. Low-pressure friction surfacing at contact pressures less than 10 MPa was studied with a view to developing a friction surfacing technology that requires simple and cheap equipment [2, 8]. Strongly bonded coatings of tool steel [8] and stainless steel [2] were successfully deposited on mild steel substrates. Friction surfacing was found to be improved by the use of an inert gas atmosphere which restricted the formation of an oxide film between the coating and the substrate, thereby affecting the bonding properties [8]. The present investigation was directed at the coating of mild steel and stainless steel on aluminium using a relatively soft aluminium 5083 matrix. The coatings thus obtained were evaluated using various surface characterization tools and mechanical tests for the integrity of the coating.

2. Experimental procedure

A vertical milling machine was adapted for the purpose of friction surfacing of stainless steel and mild steel consumable on an aluminium 5083 substrate. The consumable was mounted on a holder which was attached to the arbor of the vertical milling machine. The substrate plate was degreased, cleaned and placed in an enclosed perspex box with an opening in the top side for movement of the consumable rod as the table is moved, and was placed on the milling machine table. The consumable and the substrate were loaded together by using a pneumatic ram attached to the milling machine table. A steel starting plate of the same thickness as that of the aluminium substrate was placed next to the aluminium substrate so that the consumable first contacts the harder starting plate before a soft plasticized layer is generated. Once the loaded end of the consumable is sufficiently hot, the table can be moved in to the position to deposit the material on the substrate. Initially the table was raised until a 5 mm clearance between the consumable rod and the starting plate was obtained. The perspex box chamber was flushed with argon and the argon pressure was kept just above the atmospheric pressure to ensure an inert atmosphere. The milling machine

0022–2461

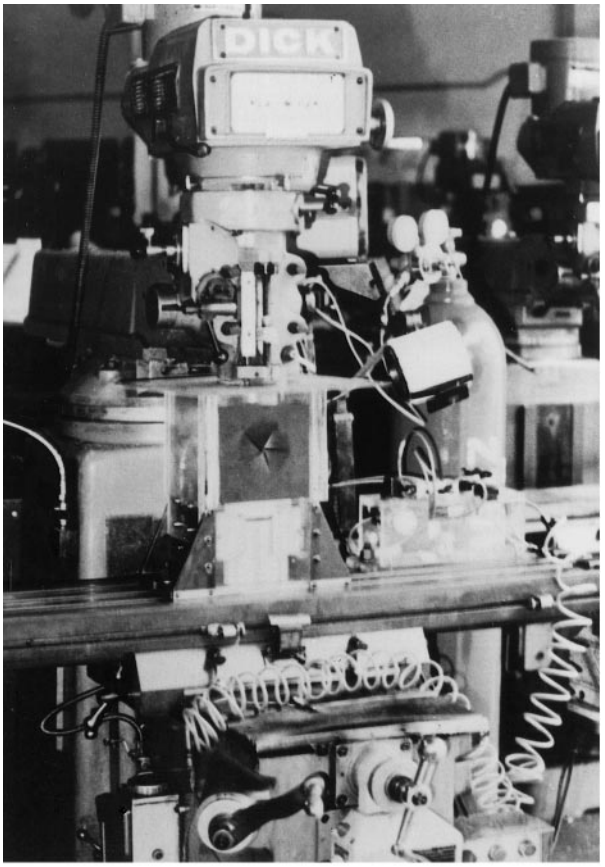

Figure 1 Friction surfacing apparatus.

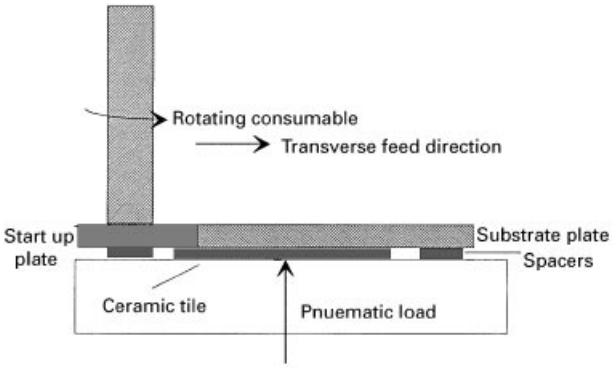

Figure 2 A schematic outline of the friction surfacing process.

was set at the required spindle speed, feed rate and compressed pressure. The pneumatic cylinder was then raised to bring the starting plate into contact with the consumable rod. Once the required heating of the loaded end of consumable rod to visible red heat is achieved, the transverse feed of the milling machine table is switched on to move the consumable rod over the aluminium substrate plate for about 60 mm. The hot consumable material plastically flows over the substrate to form a thick coating [9]. Figs 1 and 2 show photographs of the equipment and a line sketch of the friction surfacing process.

After one pass of the consumable over the substrate, the thus-coated substrate was removed from the milling machine for later examination. A feinfocus X-ray microscope and Cambridge scanning electron microscope (SEM) were used to provide interior and exterior views, respectively, of the coating. The specimens for observation under the X-ray feinfocus instrument required only limited preparation and, as a result, much of the detail i.e. structure, of the coatings was preserved which would otherwise be lost due to preparation techniques. Because steel-coated specimens were used, the voltage required to obtain the image on the fluorescent screen was high, and was varied from 55–65 kV with a filament current of approximately 55 μA to obtain the details of the coating. The X-ray images of the coatings were taken on the coating plane (i.e. X-rays were passed parallel to the coating plane in Figs 19 and 20 and normal to the plane of coating in Fig. 21, see later).

TABLE I Friction surfacing parameters for MS/SS coating on Al 5083

Material	Nominal contact pressure (MPa)	Feed rate ($mm\,s^{-1}$)	Spindle speed (r.p.m.)
SS/Al 5083	21.8	1.2	3000
SS/Al 5083	21.8	1.2	2000
SS/Al 5083	16.35	1.2	3000
SS/Al 5083	16.35	1.2	2500
SS/Al 5083	16.35	1.2	1500
SS/Al 5083	8.175	1.2	3000
SS/Al 5083	8.175	1.2	2500
SS/Al 5083	8.175	1.2	1500
MS/Al 5083	21.8	2.0	3000
MS/Al 5083	21.8	2.0	2000
MS/Al 5083	16.35	2.0	3000
MS/Al 5083	16.35	2.0	2500
MS/Al 5083	16.35	2.0	1500
MS/Al 5083	8.175	2.0	3000
MS/Al 5083	8.175	2.0	2500
MS/Al 5083	8.175	2.0	1500

The friction surfacing parameters are provided in Table I.

For SEM observation, the friction-surfaced specimens of SS on aluminium and MS on aluminium were plain polished by mounting the specimen in a plastic holder with the transverse side facing upwards. Coating integrity, i.e. the presence of porosity and gaps between the coating and the substrate, was then evaluated by SEM.

3. Results

The primary consideration of determining appropriate values of coating parameters is to find the optimum operating conditions for obtaining consistent and good coating integrity. Coating quality as a function of nominal contact pressure and speed is shown in Figs 3 and 4.

It is evident from Figs 3 and 4 that at lower axial pressures and speeds, SS 304 is not effectively coated. It was also found that lower nominal contact pressures with lower speeds led to a drilling effect by SS 304 on the aluminium substrate plate.

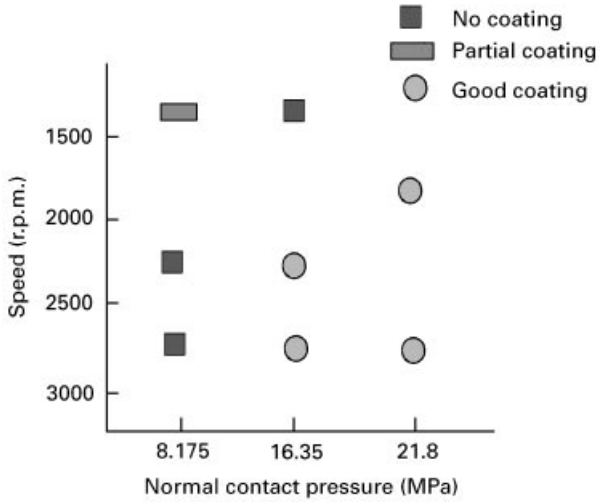

Figure 3 Effect of sliding speed and normal contact pressure on the coating integrity of MS.

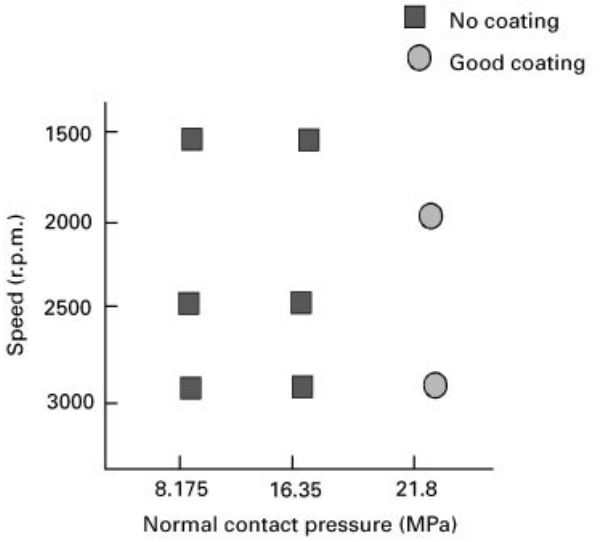

Figure 4 Effect of sliding speed and normal contact pressure on the coating integrity of SS.

3.1. Scanning electron micrographs

Figs 5–7 show interface of the coating of MS and aluminium in the samples prepared using a spindle speed of 3000 r.p.m. and a nominal contact pressure of 21.8 MPa. It can be observed from Fig. 5 that mechanical locking of the contacting materials had occurred. It shows no clear evidence of the formation of an intermetallic phase at this magnification and the coating was observed to be free of any defects at the interface line at a magnification of $\times 45.4$. Fig. 6 shows the clear evidence of mechanical locking between the substrate and the coating and a gap of around 5 μm along the interface in the substrate. Fig. 7 indicates the evidence of transfer of aluminium from the substrate to the steel-coating surface, subsurface failure in the aluminium matrix and cracking of subsurface due to shear bands generated due to transfer of aluminium. The matrix failure can be attributed due to the transfer of aluminium on to steel and the generation of shear bands to accommodate the sliding

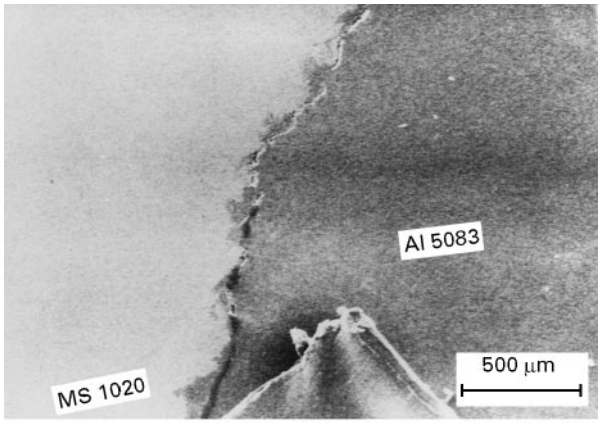

Figure 5 Scanning electron micrograph of the interface of MS/Al 5083 at a magnification of $\times 45.4$.

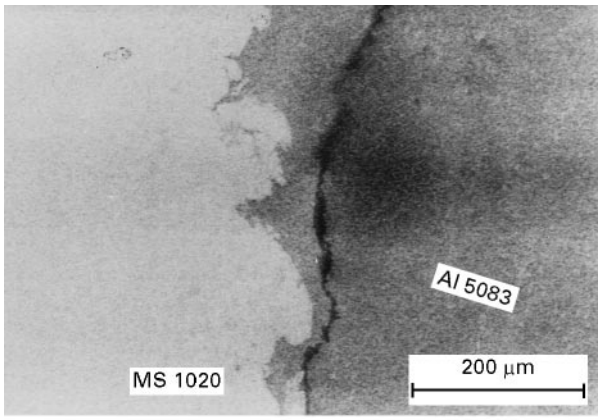

Figure 6 Scanning electron micrograph of the interface of MS/Al 5083 at a magnification of $\times 161$.

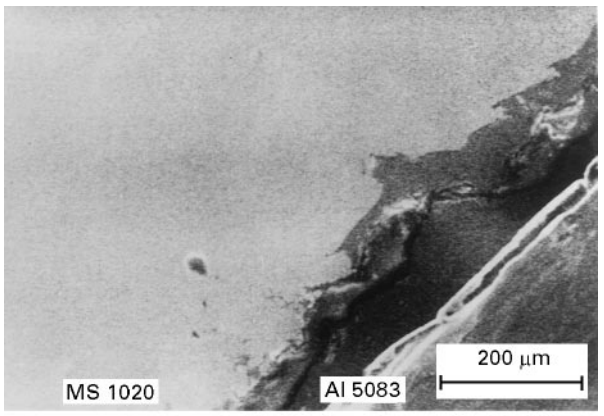

Figure 7 Scanning electron micrograph of the interface of MS/Al 5083 at a magnification of $\times 203$.

which finally develops as a crack when the shear strength of the subsurface is exceeded [9–14].

Figs 8–10 show scanning electron micrographs of the coating of SS304 on aluminium 5083 matrix at a spindle speed of 3000 r.p.m. and nominal contact pressure of 21.8 MPa. It is evident from the figures that the coating had defects, such as gaps, between the coating and substrate and cracks in the coating which were invisible to the naked eye. No clear evidence of

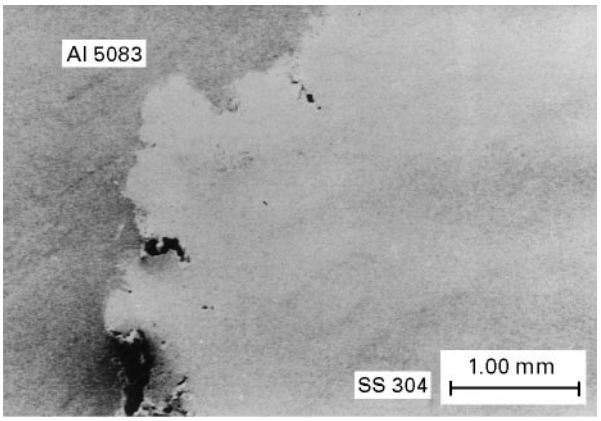

Figure 8 Scanning electron micrograph of the interface of SS/Al 5083 at a magnification of ×36.

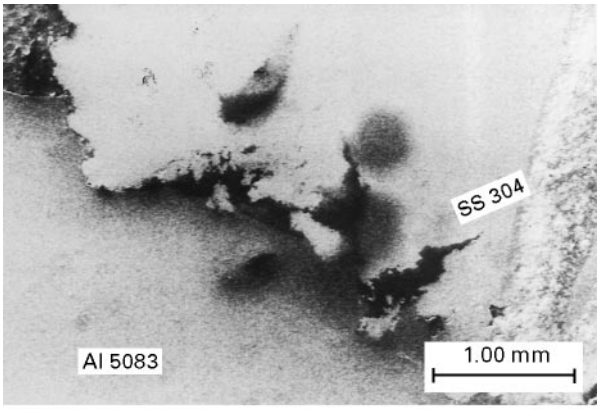

Figure 9 Scanning electron micrograph of the interface of SS/Al 5083 at a magnification of ×40.

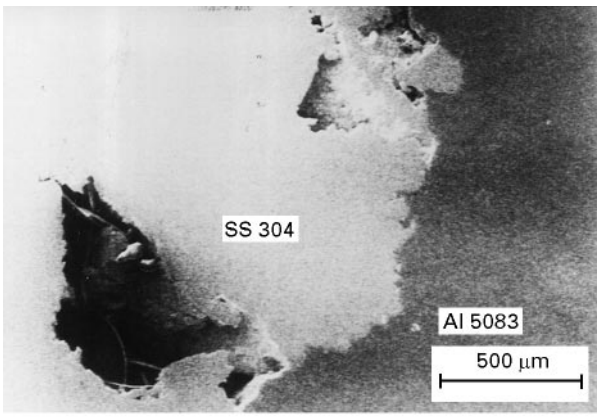

Figure 10 Scanning electron micrograph of the interface of SS/Al 5083 at a magnification of ×50.

mechanical locking, as observed for MS coatings, was obtained for the SS friction surfaced specimens. It can be clearly observed from Fig. 8 that the SS coating has spread over the aluminium substrate and no clear interfacial line is seen, thereby masking the type of bonding at the interface. It also shows an uneven surface of SS coating together with tearing of the coating at the interface with a cavity of approximately 100 μm size. Fig. 9, taken at a slightly higher magnification (×40) along the interface at a different location, indicated that the coating had cracks propagating from the interface towards the centre of the coating. Fig. 10 shows the magnified (×50) micrograph of the coating at a different location where a large cavity with a filament-like structure is seen. It is hypothesized that the filament-like structure is due to the layers peeling off the consumable rod (delamination) being rolled into thin filaments as the linear feed is activated during the friction surfacing process. In general, the material is not released as a continuous flow during friction surfacing, but instead is released as discrete lameller layers. These filaments may then have bonded together due to heat and pressure to form a coating. The reason for the uneven surface observed in Fig. 8 is probably due to the rolling effect of SS. Aluminium had also probably undergone plastic deformation at the boundary to accommodate plastically flowing SS. Detachment of SS was also observed at the boundary of the coating thus indicating weak bonding of the filaments. The degree of plasticity attained on frictional heating of MS may be higher than the degree of plasticity attained with SS, which could have been the reason for better coating integrity of MS coatings. The fact that MS could be coated even at a lower axial pressure and speeds is further evidence of the hypothesis.

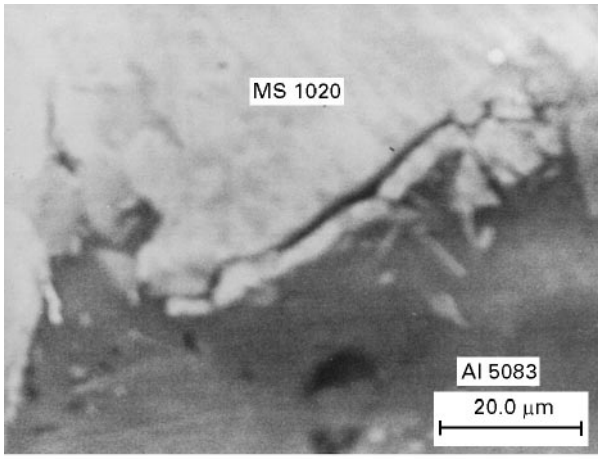

Figure 11 Scanning electron micrograph of the interface of MS/Al 5083 at a magnification of 2.09k.

Figs 11 and 12 show the secondary and the X-ray mapped images of MS/Al interface. It is seen that there is a third phase of Fe–Al (which was confirmed by EDAX spot analysis of the interface) present at the interface separating the aluminium and the mild steel. Figs 13 and 14 (FeK_α and AlK_α dot-mapped images, respectively) also confirm that the mild steel and aluminium did mix along the interface forming a third phase (Fe_3Al).

Figs 15 and 16 show the secondary and the X-ray mapped images of the SS/Al interface. It is evident that no third phase formed during surfacing and a clear interface is seen. Dot mapping using the FeK_α and AlK_α radiation was performed to confirm the above observation and the same is depicted in Figs 17 and 18. It can be clearly seen that there has been no mixing at the interface.

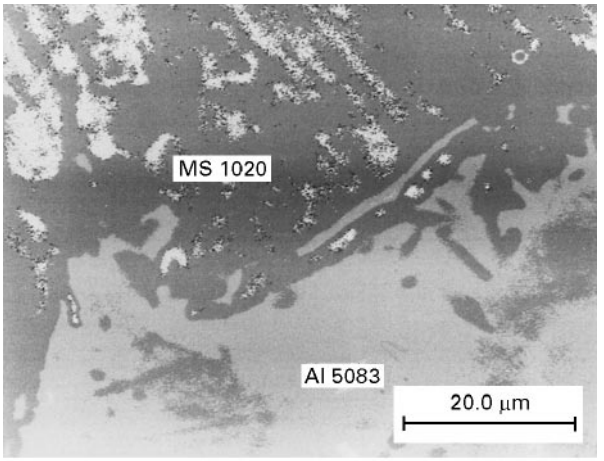

Figure 12 Corresponding X-ray mapped image of the MS/Al 5083 interface at a magnification of 2.09k.

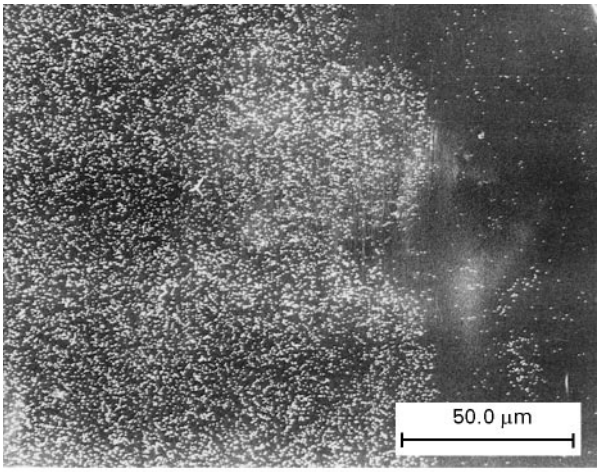

Figure 13 X-ray dot-mapped image of MS/Al 5083 interface using FeK_α radiation.

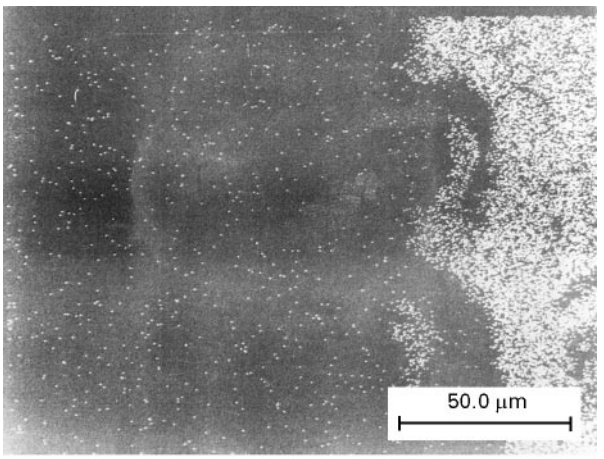

Figure 14 X-ray dot-mapped image of MS/Al 5083 interface using AlK_α radiation.

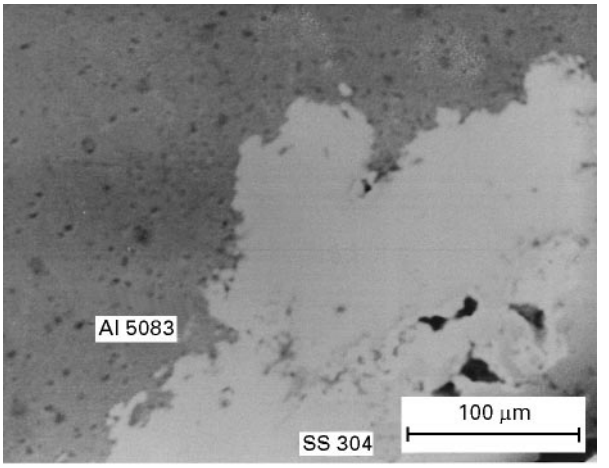

Figure 15 Scanning electron micrograph of the interface of SS/Al 5083 at a magnification of $\times 232$.

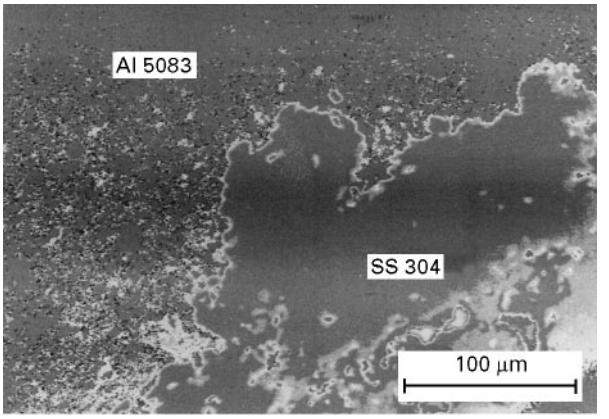

Figure 16 Corresponding X-ray mapped image of the MS/Al 5083 interface at a magnification of $\times 232$.

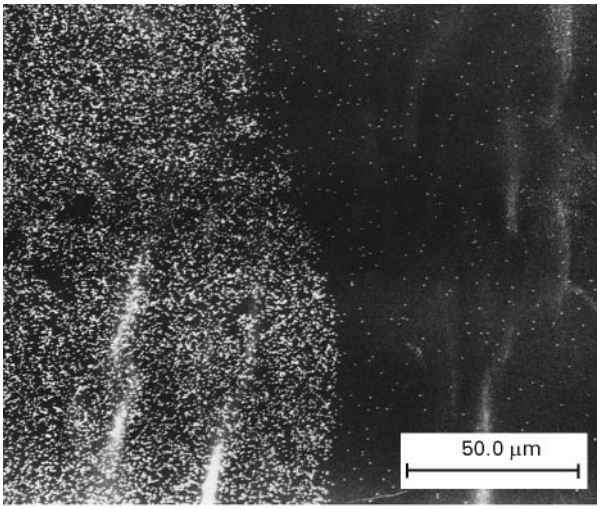

Figure 17 X-ray dot-mapped image of SS/Al 5083 interface using FeK_α radiation.

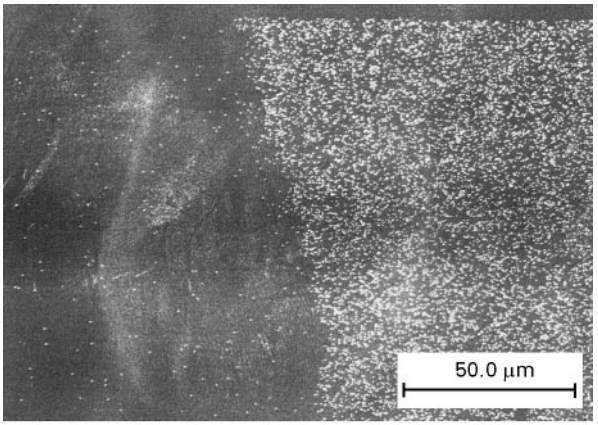

Figure 18 X-ray dot-mapped image of SS/Al 5083 interface using AlK_α radiation.

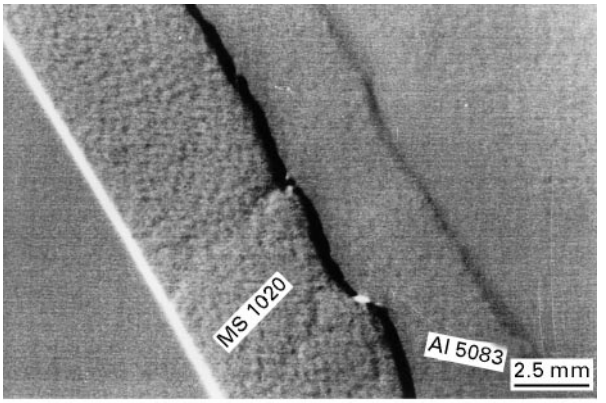

Figure 20 Normal X-ray fluoroscopic image of the MS/Al 5083 interface mask processed using a three-dimensional difference function.

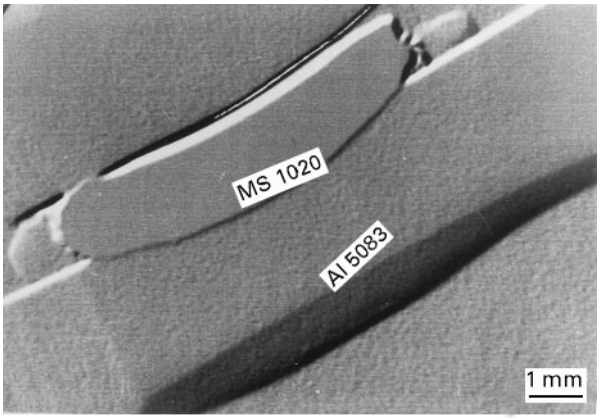

Figure 19 Transverse X-ray fluoroscopic image of the MS/Al 5083 interface mask processed using a three-dimensional difference function.

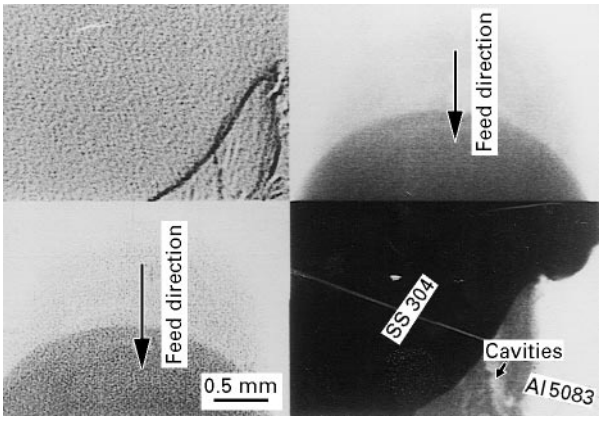

Figure 21 Normal X-ray fluoroscopic image of the SS/Al 5083 interface mask processed using a three-dimensional difference function.

3.2. X-ray fluoroscopic images

Fig. 19 shows the X-ray image of the coating of mild steel on aluminium 5083 alloy viewed from the side along the length of the coating. A thick coating is observed and coating defects are not observed when viewed from the side (X-rays were passed parallel to the coating plane, i.e. interface). The aluminium was found to have a bulged edge on the side opposite to the coating, indicating the force was on the higher side to create a bending moment sufficient to cause bulging or bending of aluminium. It is also evident that the deposit had penetrated deeper at the centre of the application of normal load while at the edge of the deposit, coating quality was not uniform and the depth of penetration was less. This could possibly be due to higher load and lesser frictional heat dissipation from the centre, compared to the edges.

Fig. 20 shows the X-ray image of coating of MS on to Al 5083 viewed from the top along the side. It is evident from Fig. 20 that steel has ploughed into aluminium and formed a mechanical lock. The layered structure is evident and deformation of aluminium is also observed along the coating to accommodate steel flow.

Fig. 21 shows the mask-processed X-ray images of the SS 304 coating on Al 5083. The first quadrant image shows the three-dimensional layered structure and the second quadrant image shows the integrated image towards the edge of the coating. It can be clearly seen that the coating has been deposited in layers and the thickness of the layer is lesser towards the edge/end of the coating. When the feed of the stainless steel was stopped some amount of material has flowed plastically, thus spreading further, and the coating thickness is lower when the movement of the feed stock was stopped because there was no further supply of material over this region. The loss of thickness is confirmed by the third quad image which, in addition to integration, has been mask-processed to reveal more details. It can be clearly seen from these images that flow of material is less, cavities are found, towards the end of the coating, facilitating a greater penetration of X-rays through the surface.

4. Discussion

A strong influence of consumable rotation speed and load on coating quality was observed. Both stainless steel and mild steel did not coat effectively on the

aluminium substrate at low speeds and low loads. The MS could, however, be reasonably coated at a lower speed but higher feed rate than SS. The inability to obtain good coating of MS and SS consumables at lower loads and speeds could be due to insufficient frictional heat generated to initiate plastic flow of material. The hardness level was approximately 183 HB at room temperature for stainless steel and 143 HB for mild steel. The finding that mild steel could be coated at comparatively lower loads and higher feed rates could be due to the lower hardness than SS which may have facilitated easier flow of material once the plasticizing temperature of the steel is obtained. It can be observed from the X-ray images that coatings, as observed in the cross-section, exhibit good bonding by mechanical interlocking. It can also be seen that bending of aluminium occurs at the centre of the application of the load, i.e. where the depth of coating is higher, indicating the axial pressure of the consumable was high enough to cause bending of the substrate.

The mechanical locking of MS on the aluminium substrate observed in Fig. 5 is due possibly to the surface-localized deformation of aluminium to accommodate the plastically flowing mild steel and the MS asperity. Higher magnifications views shown in Figs 6 and 7 provide an example where the crack in the substrate matrix is the result of the adhesion and ploughing present in friction surfacing leading to the formation of shear bands in the matrix. When the deformation stress of the shear bands exceeds the shear strength of the matrix, crack formation and propagation occurs. For stainless steel, the hardness difference between MS and SS ensures that the stainless steel does not flow as easily as observed in the case of MS. This can be inferred from the coating parameters required for SS and MS coatings as discussed above. Further confirmation of the role of hardness is provided by X-ray mapped images of MS on Al 5083 and SS on Al 5083 shown in Figs 11–15, where a clear interfacial line is observed between SS and aluminium whereas for MS and aluminium there is evidence of a thin interfacial phase. The absence of a phase formation at the SS/Al interface could be due to the alloying additions which require higher temperatures for a reaction product to be formed. Plastic deformation and heat encourage the chromium and other alloying additions to migrate to the surface and act as a reaction barrier between steel and aluminium. The coating integrity is also poor in comparison to the MS/Al coating which may be due to the alloying additions in stainless steel contributing to the strength and higher hardness, thereby reducing plasticity at the temperature achieved by frictional heating.

The basic mechanisms found to be operative when MS and SS were friction surfaced on aluminium are described below.

During rotation of the consumable over the stationary substrate, the mild steel rod was found to deposit by direct plastic deformation and flow over the substrate. For stainless steel the coating appears to be formed by delamination and rolling of delaminated steel surface on the substrate. This behaviour is better

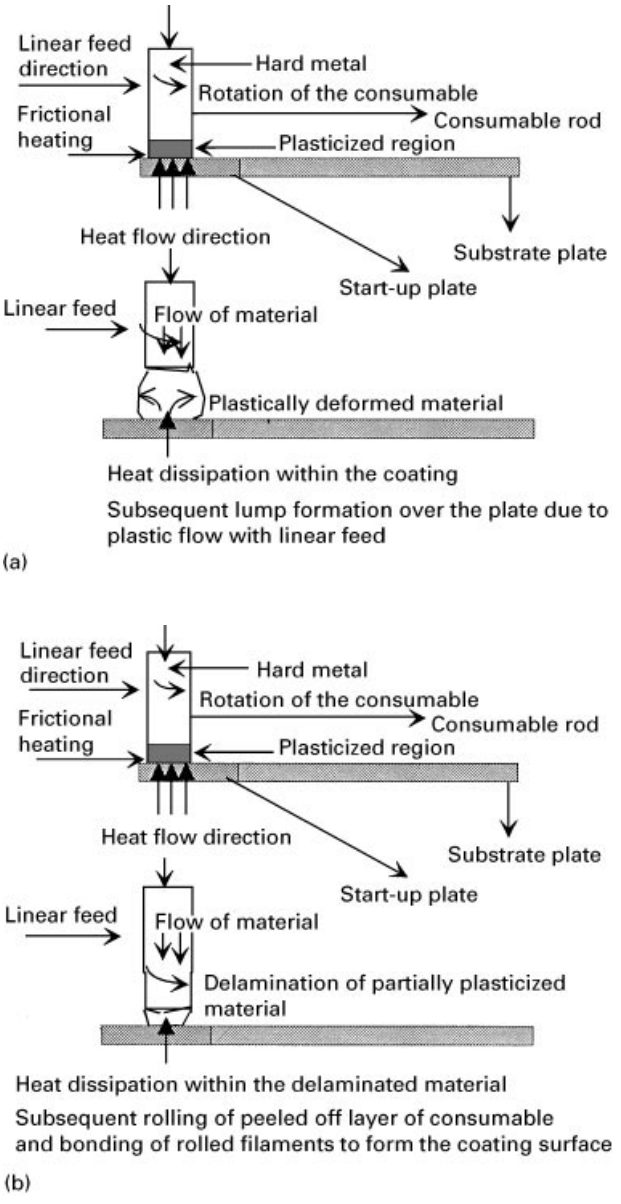

Figure 22 Possible mechanisms of friction surfacing in (a) an MS consumable, and (b) SS 304 consumable.

visualized with the help of two different figures (Figs 22a and b). In the case of mild steel, the frictional heat generated between the surfaces caused localized softening and plasticized the mild steel. As the heat flow to the atmosphere is blocked by the plasticized consumable rod (which acts as a barrier for flow of heat to the sides), the heat thus generated due to friction is conducted through the consumable and during this process it further softens the consumable rod, thereby facilitating downward flow of material and consumable rod. This effect, combined with the linear feed of the consumable, leads to the formation of plastic flow of steel on the surface. The aluminium which was also frictionally heated was deformed and displaced by the plasticized steel.

The stainless steel consumable surface appears to delaminate and the delaminated layer rolls over before attaining the necessary plasticity for flowing over the substrate under the action of external linear feed. This leads to formation of a thin filament-like structure

which, under the action of friction surfacing pressure and heat, bonds together forming an uneven coating over the aluminium. The filament structure is confirmed from the scanning electron micrographs which show a filament-like structure as well as an uneven coating surface. Evidence for the model is found in the Fig. 22a and b.

5. Conclusions

1. The above study indicates that friction surfacing could be used as a method for obtaining coatings of dissimilar materials.

2. Mild steel is more effectively deposited by friction surfacing than stainless steel. Stainless steel requires a higher nominal contact pressure than mild steel to produce a consistent coating. This difference in nominal contact pressure may be due to lesser plasticity of stainless steel.

3. The mild steel coating had better bonding than the stainless steel coating, which may be due to a lower hardness and plasticizing temperature which facilitates plastic flow and leads to intimate contact between coating and deposit.

4. The chromium and other alloying elements in stainless steel appear to block the formation of the interfacial phase.

5. The stainless steel appears to be deposited from rolls of material trapped between the consumable and substrate.

Acknowledgements

The authors acknowledge with thanks the support of the School of Mechanical and Production Engineering, Nanyang Technological University. Mr Chua Meng Kuan and Mr Er Seng Koon are thanked for experimental help.

References

1. HANS KLOPSTOCK and A. R. NEELANDS, An improved Method of Joining and Welding Metals, U.K. Patent No. 572, 789, 17 Oct., 1941.
2. P. LAMBRINEAS, B. M. JENKINS and E. D. DOYLE, in "Institute of Engineers, Australian Tribology Conference", 3–5 December 1990, Brisbane, Australia edited by D. Scott (Institute of Engineers Australian National Conference Publication no. 90/14 (1990) p. 12.
3. KH. A. TYAGAR, *Weld. Prod.* **10** (1959) 23.
4. R. I. ZAKSON and F. G. TURKIN, *Avt. Svarka* **3** (1965) 48.
5. W. M. THOMAS and S.B. DUNKERTON, *Weld. Inst. Res. Bull.* **25** (1984) 327.
6. W. M. THOMAS, E. D. NICOLAS and S. B. DUNKERTON, The Welding Institute Research Report, no. 236/1984, Abington Hall, Abington, Cambridge, UK (1984).
7. W. M. THOMAS, "Proceedings of the First International Conference on Surface Engineering", Paper 66 (The Welding Institute, Abington, UK, 1987) p. 261.
8. B. M. JENKINS and E. D. DOYLE in "Proceedings of the International Tribology Conference", Melbourne, Australia edited by E. Hennings (Institution of Engineers Australian National Conference Publ 87/18 (1987) p. 87.
9. A. W. BATCHELOR and S. JANA, *J. Mater. Process. Technol.*, **57** (1996) 172.
10. K. H. ZUM GAHR, "Microstructure and Wear of Materials" (Elsevier, Amsterdam, 1987).
11. E. M. KOPALINSKY and P. B. OXLEY, in "Proceedings of the International Tribology Conference-Austrib 94", edited by G. Stachowiak (University of Western Austalia, Perth, 1994).
12. D. H. BUCKLEY, "Surface Effects Adhesion Friction and Lubrication" (Elsevier Science, Amsterdam, 1981).
13. D. KUHLMANN-WILSDORF, in "Proceedings of the International Conference on Wear of Materials", edited by K. C. Ludema (ASME, New York, 1983) p. 402.
14. ZHOU ZEHUA and CHEN PING, *Wear* **128** (1988) 173.

Received 20 March
and accepted 3 October 1996